JACS
JOURNAL OF THE AMERICAN CHEMICAL SOCIETY

Article

pubs.acs.org/JACS

Self-Assembly of Concentric Hexagons and Hierarchical Self-Assembly of Supramolecular Metal–Organic Nanoribbons at the Solid/Liquid Interface

Ming Wang,[†,‡] Kun Wang,[§] Chao Wang,[†] Mingjun Huang,[∥] Xin-Qi Hao,[*,⊥] Ming-Zhan Shen,[⊥] Guo-Qing Shi,[#,⊥] Zhe Zhang,[†,▽] Bo Song,[†] Alejandro Cisneros,[†] Mao-Ping Song,[⊥] Bingqian Xu,[*,§] and Xiaopeng Li[*,†]

[†]Department of Chemistry and Biochemistry & Materials Science, Engineering, and Commercialization Program, Texas State University, San Marcos, Texas 78666, United States

[‡]State Key Laboratory of Supramolecular Structure and Materials, College of Chemistry, Jilin University, Changchun, Jilin 130012, People's Republic of China

[§]Single Molecule Study Laboratory, College of Engineering and Nanoscale Science and Engineering Center, University of Georgia, Athens, Georgia 30602, United States

[∥]Department of Polymer Science, College of Polymer Science and Polymer Engineering, The University of Akron, Akron, Ohio 44325, United States

[⊥]College of Chemistry and Molecular Engineering, Zhengzhou University, Zhengzhou 450001, People's Republic of China

[#]College of Food and Biological Engineering, Zhengzhou University of Light Industry, Zhengzhou 450002, People's Republic of China

[▽]College of Chemistry, Central China Normal University, Wuhan 430079, People's Republic of China

Supporting Information

ABSTRACT: In an effort to exert more precise control over structural features of supramolecules, a series of giant concentric hexagons were assembled as discrete structures using tetratopic terpyridine (tpy) ligands. In preparation of tetratopic ligand, pyrylium and pyridinium salts chemistry significantly facilitated synthesis. The key compounds were obtained by condensation reactions of pyrylium salts with corresponding primary amine derivatives in good yields. These discrete metallo-supramolecular concentric hexagons were fully characterized by NMR, ESI–MS, TWIM–MS, and TEM, establishing their hexagon-in-hexagon architectures. The combination of different tetratopic ligands also assembled hybrid concentric hexagons with increasing diversity and complexity. Furthermore, these concentric hexagon supramolecules with precisely controlled shapes and sizes were utilized as building blocks to hierarchically self-assemble supramolecular metal–organic nanoribbons (SMON) at solid–liquid interfaces. Ambient STM imaging showed the formation of long 1D SMON rather than 2D assembly on the basal plane of highly oriented pyrolytic graphite (HOPG) surface after simple dropcasting of the solution of preassembled concentric hexagons onto a freshly cleaved surface of HOPG. This wet chemical method based on self-assembly may offer simple, economical, and scalable routes to deliver complex materials.

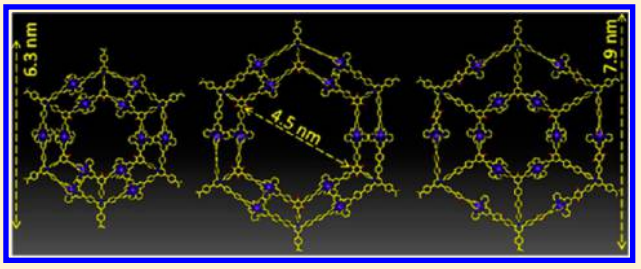

INTRODUCTION

Nature has created a myriad of unique cyclic molecules with different length scales and complexity, ranging from benzene and pyrrole to porphyrin family, such as heme, vitamin B12, or chlorophylls, from cyclodextrins family to cyclic protein complexes, such as light-harvesting complex and the family of nucleoside triphosphate helicases.[1] Cyclic molecules have fascinated chemists for many years in both fundamental study and applied research.[2] Exploring such cyclic structures is often hampered by their challenging and low yielding synthesis, which gives mixtures of rings with different sizes as a result of entropically unfavored cyclization. Synthesizing preorganized building blocks and applying template-directed cyclizations reduced entropic and enthalpic barriers to cyclization, and thus significantly increased the yields and gave macrocycles with larger cavities.[3] It, however, still requires sophisticated design and multistep synthesis to prepare templates.

Alternatively, the emergence of supramolecular chemistry acting as a powerful tool to mimic nature's activities had a profound effect on the preparation of macrocycles.[4] Particularly, metal-mediated self-assembly has received considerable attention

Received: May 13, 2016
Published: July 5, 2016

DOI: 10.1021/jacs.6b04959
J. Am. Chem. Soc. 2016, 138, 9258–9268

in constructing various supramolecular structures with precise geometries and sizes due to the highly directional and predictable feature of metal coordination.[5] Obstacles do exist, however, in self-assembly of metallo-macrocycles because the bending of ditopic organic ligands and distortion of coordination geometry can accommodate significant structural strain and lead to unexpected macrocycles.[6−9] The question brought up in the field is how we can improve the design of metallo-macrocycles to reach discrete structures.

The success of 3D self-assembly using naked metal ions by Stang,[10] Fujita,[11] Nitschke,[12] Shionoya,[13] Clever,[14] and others[15] inspired us to rethink the design of 2D macrocycles. In many cases of 3D self-assembly, each metal ion provides multiple (≥3) interactions with ligands, which act cooperatively and yield stable supramolecular architectures. A high "density of coordination sites" (DOCS) resulted from multivalency[16] should play a critical role in designing and guiding the topologies of final assemblies. Directed by increasing the overall DOCS of macrocycles, herein we describe the design and self-assembly of a concentric hexagon system, hexagon-in-hexagon, using a series of tetratopic ligands based on 2,2′:6′,2″-terpyridine[17] (tpy). If a tetratopic ligand was synthesized with suitable geometry as shown in Scheme 1, we may obtain a discrete hexagon-in-hexagon with high DOCS based on geometry and topology analysis, while a high generation of concentric hexagon is also possible if a hexatopic ligand is employed for self-assembly. Furthermore, if the first level of assembly is assumed as the spontaneous formation of metal−ligand bonds to generate discrete cores, hierarchical self-assembly driven by multiple intermolecular interactions (e.g., $\pi-\pi$ stacking, CH$-\pi$ interactions, and hydrogen bonds) and/or molecule−substrate interactions in the second level should be able to deliver complex materials.[18] Such hierarchically formed architectures may exhibit unique properties and functions that are not displayed by their individual components. On the basis of this motivation, we attempted to use preassembled supramolecular concentric hexagons with precisely controlled shapes and sizes as building blocks to assemble supramolecular metal−organic nanoribbons (SMON) at solid−liquid interfaces.

Scheme 1. (A) Hexagon Assembled by Conventional Ditopic tpy Ligands; (B) Hexagon-in-Hexagon Structure Assembled by Tetratoptic tpy Ligands; and (C) A Representative High Generation of Concentric Hexagon

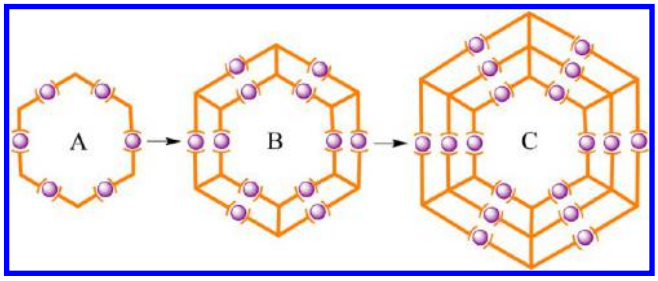

RESULTS AND DISCUSSION

Synthesis and Self-Assembly of Concentric Hexagons [$Zn_{12}LA_6$] and [$Zn_{12}LB_6$]. In an effort to exert more accurate control over structural features of supramolecules, we designed and evaluated a large pool of tetratopic tpy ligand candidates with different geometry and linkers for the self-assembly of concentric hexagons with all rigid aromatic backbones. According to molecular modeling, the structures of ligands **LA**−**LD** are the optimal ones to generate concentric hexagons with minimum geometric constraints as shown in Figure 1. As compared to recently reported sphere-in-sphere[11c] and ring-in-ring[3e,19] supramolecular architectures with flexible linkers between inner and outer layers, our design of hexagon-in-hexagon structures with all aromatic backbone required more precise preorganization of the entire structure because of their highly structural homogeneity. It is also expected that concentric hexagons with rigid geometry may enhance the interaction with surface, and thus hierarchically assemble a specific pattern, for example, metal−organic nanoribbons. Note that the octahedral coordination geometry of the tpy-metal(II)-tpy motif could be severely distorted due to the short distance between the inner and outer rims. If distortion of octahedral coordination exists, the two terpyridine units bound to each zinc center may have enhanced interactions with a specific surface to assist hierarchical assembly. Such design without flexible linkers, however, posed a great challenge in the synthesis of tetratopic ligands by introducing a different tpy moiety into the inner and outer rims of concentric hexagons. In our synthesis, the condensation reaction of pyrylium salts with primary amines was employed to dramatically simplify the preparation of multitopic ligands. Moreover, the resulted tetratopic tpy ligands based on pyridinium salts also hold

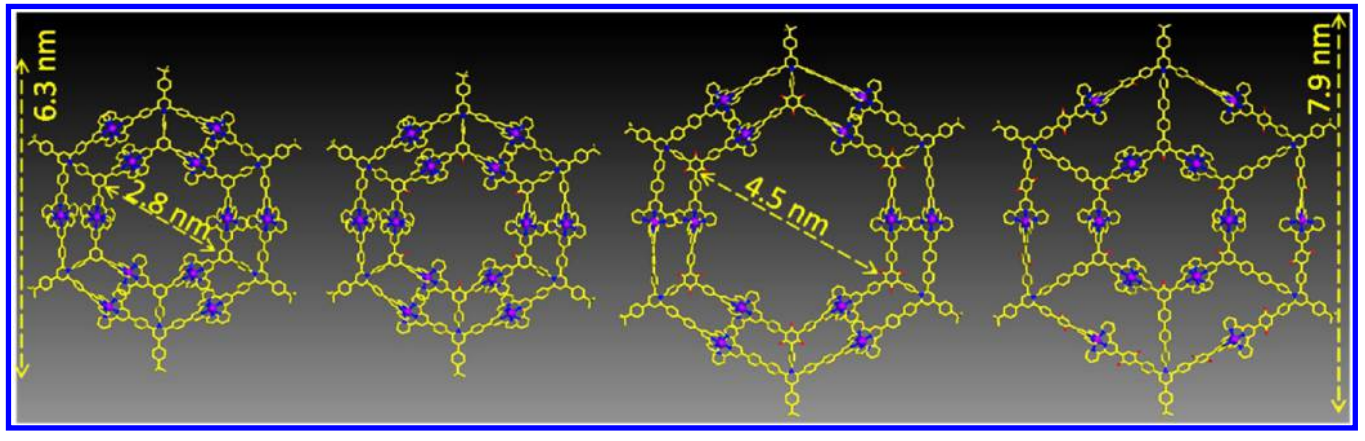

Figure 1. Energy-minimized structures of complexes [$Zn_{12}LA_6$], [$Zn_{12}LB_6$], [$Zn_{12}LC_6$], and [$Zn_{12}LD_6$] (left to right). The alkyl chains are omitted for clarity in the molecular modeling.

DOI: 10.1021/jacs.6b04959
J. Am. Chem. Soc. 2016, 138, 9258−9268

particular promise for future studies of redox, electro-optical, and photophysical properties.[20]

We initiated this study from the synthesis of tetratopic tpy ligands **LA** and **LB**. The condensation reactions between pyrylium salt **1** and primary amine **7** or **8** simplified the synthesis process with a decent yield of pyridinium salt **9** and **10**, respectively.[20b,21] **LA** and **LB** were then synthesized by Suzuki coupling reaction of pyridinium salt **9** or **10** with short tpy head **2** and purified by column chromatography (Scheme 2). For self-assembly,

Scheme 2. Synthesis of Ligands LA and LB and Self-Assembly of Concentric Hexagons $[Zn_{12}LA_6]$ and $[Zn_{12}LB_6]$[a]

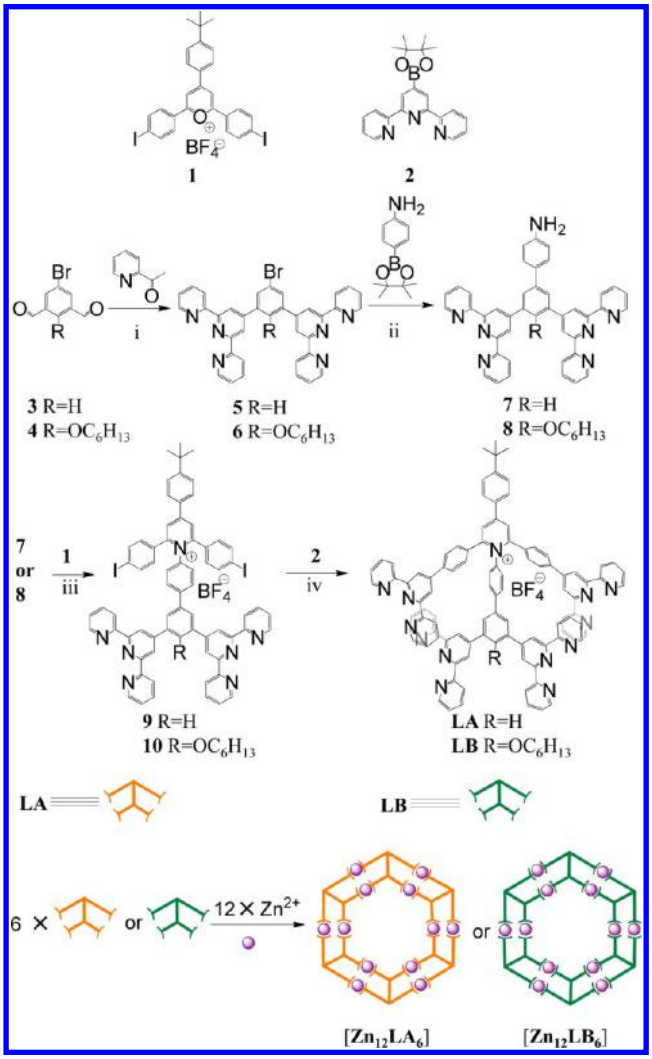

[a](i) Ethanol, NaOH, $NH_3{\cdot}H_2O$; (ii) $Pd(PPh_3)_2Cl_2$, K_2CO_3, H_2O, toluene; (iii) NaOAc, ethanol; (iv) $Pd(PPh_3)_2Cl_2$, K_2CO_3, DMSO, H_2O.

a stoichiometric ratio (1:2) of **LA** and $Zn(NO_3)_2{\cdot}6H_2O$ was mixed in $CHCl_3$/MeOH at 50 °C for 8 h, followed by the addition of an excess of NH_4PF_6 salt to give a white precipitate $[Zn_{12}LA_6]$ (yield 90%) after a thorough washing with water. In this process, NO_3^- ions were converted to PF_6^- counterions.

The self-assembly with $[Zn_{12}LA_6]$ composition was measured by ESI−MS and traveling-wave ion mobility-mass spectrometry (TWIM−MS)[22,23] (Figure S5) with a molecular weight of 13 759.6 Da. The experimental isotopic distributions were in good agreement with the calculated distributions. As yet, the low solubility of this complex obstructed further characterization by NMR to confirm the so-formed structure. After introducing a hexyloxy chain ($-OC_6H_{13}$) into the inner rim of the concentric hexagon, ligand **LB** was prepared and characterized by NMR and MALDI-TOF mass spectrometry (Figures S11 and S15). The solubility of the corresponding concentric hexagon $[Zn_{12}LB_6]$ was significantly improved to facilitate further characterization by NMR.

^{1}H NMR spectra of ligand **LB** and complex $[Zn_{12}LB_6]$ were shown in Figure 2. There are two sets of tpy signals found in

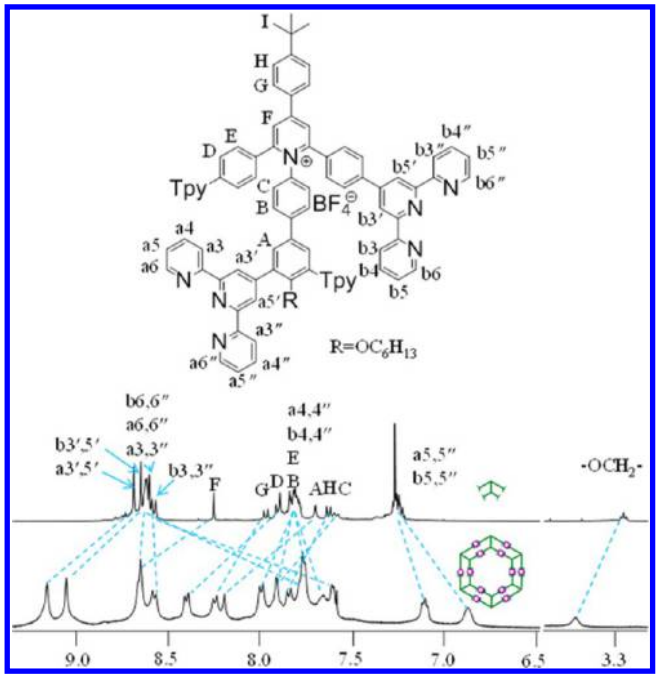

Figure 2. ^{1}H NMR spectra (400 MHz) of ligand **LB** in $CDCl_3$ and complex $[Zn_{12}LB_6]$ in CD_3CN. The term "tpy" was used to replace the terpyridine structure.

^{1}H NMR of **LB** judged by the characteristic peaks of a3′,5′ and b3′,5′. These two groups of ^{1}H signals from tpy were confirmed by 2D-COSY results (Figures S13 and S14). Other proton signals of tpy rings are overlapped in the aromatic region. After complexation, broad ^{1}H NMR signals were observed for complex $[Zn_{12}LB_6]$, due to low tumbling motion on the NMR time scale,[11b] suggesting that a very large complex was assembled. Both the a3′,5′-tpy and the b3′,5′-tpy protons were significantly shifted to downfield, mainly attributed to the lower electron density upon coordination with metal ions. On the contrary, all 5 and 6 positions of pyridine were shifted to upfield, especially for b6,6″ position proton ($\Delta\delta$ = 1.0 ppm), as a consequence of the electron shielding effect.[24] The proton signals of the alkoxy chain ($-OCH_2-$) showed a single set of peak and the expected ratio with aromatic protons, suggesting the possibility of forming a single component after self-assembly instead of random oligomerized products. Note that the assignment of proton signals is facilitated by 2D-COSY NMR (Figure S29).

ESI−MS and TWIM−MS provided conclusive evidence for the clean formation of expected assemblies.[22] In ESI−MS (Figure 3A), one prominent set of peaks with charge states from 8+ to 20+ was observed due to the loss counterions, and each peak closely matched the corresponding simulated isotope pattern of $[Zn_{12}LB_6]$ (Figure S2) for the expected hexagon-in-hexagon structure with a molecular weight of 14 360.1 Da.

DOI: 10.1021/jacs.6b04959
J. Am. Chem. Soc. 2016, 138, 9258−9268

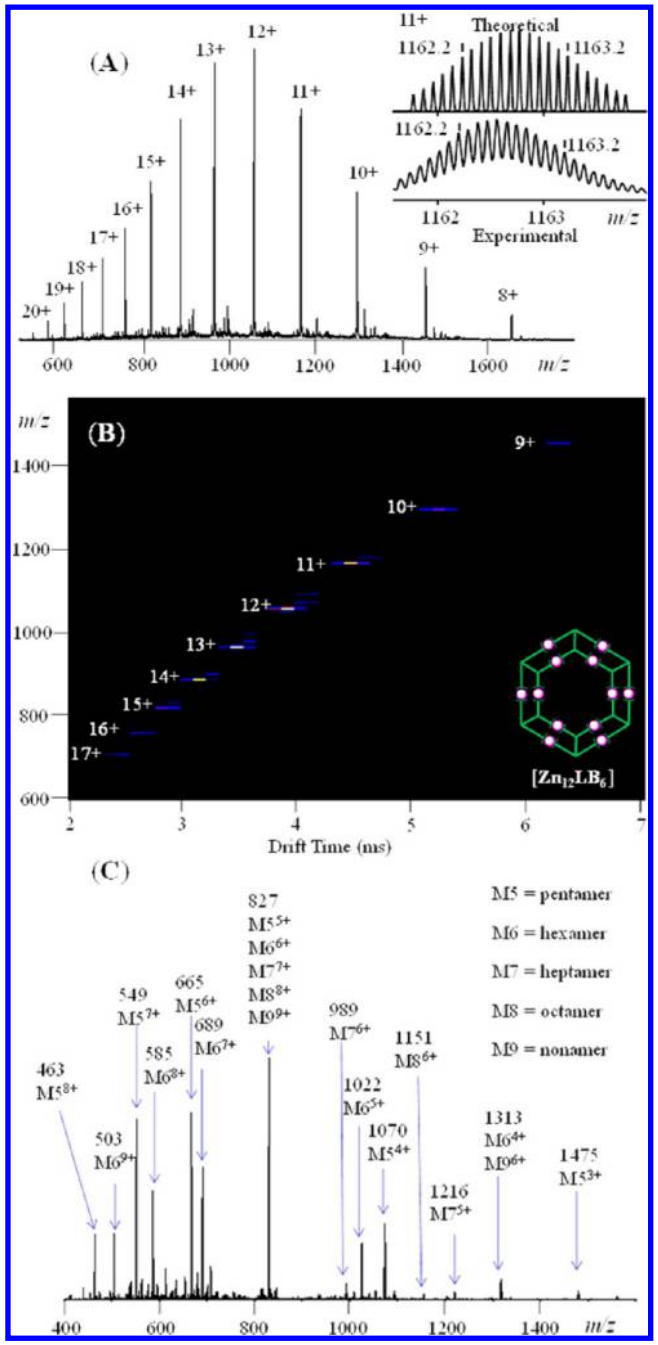

Figure 3. (A) ESI−MS and (B) 2D ESI−TWIM−MS plot (m/z vs drift time) of complex [$\mathbf{Zn_{12}LB_6}$]. (C) ESI−MS of multiple macrocycles assembled by ditopic ligand **5** with Zn(II).

In further characterization, TWIM−MS was introduced as the advanced level of MS analysis to separate any superimposed fragments and detect the possible presence of overlapping isomers or conformers. TWIM−MS is an effective approach to determine the analytes' mass, charge, and shape by analyzing the drift time of ions through ion-mobility separation combined with mass spectrometry.[22,23] Notably, each charge state of [$\mathbf{Zn_{12}LB_6}$] has a narrow drift time distribution, indicating this complex is a discrete and rigid assembly without other isomers or structural conformers.

As a comparison, ditotpic ligands **5** and **6** were also mixed with $Zn(NO_3)_2{\cdot}6H_2O$ under the same self-assembly procedure. Indeed, as was already reported,[23,25] multiple macrocycles (i.e., petamer to nonamer) rather than single hexagon were detected in ESI−MS (see Figures 3C and S41). All of these results suggest that increasing DOCS within 2D structure will help to generate single assembly by providing more geometric constraints and excluding the formation of other macrocyclic structures.

Synthesis and Self-Assembly of Concentric Hexagons [$\mathbf{Zn_{12}LC_6}$] and [$\mathbf{Zn_{12}LD_6}$]. Encouraged by the success of concentric hexagons [$\mathbf{Zn_{12}LA_6}$] and [$\mathbf{Zn_{12}LB_6}$], we added one extra phenyl group into each arm of original tetratopic ligands to prepare ligand **LC** with a longer arm, but maintained the single phenyl spacer between the inner and outer rims (Scheme 3).

Scheme 3. Synthesis of Ligand LC and Self-Assembly of Concentric Hexagon [$\mathbf{Zn_{12}LC_6}$][a]

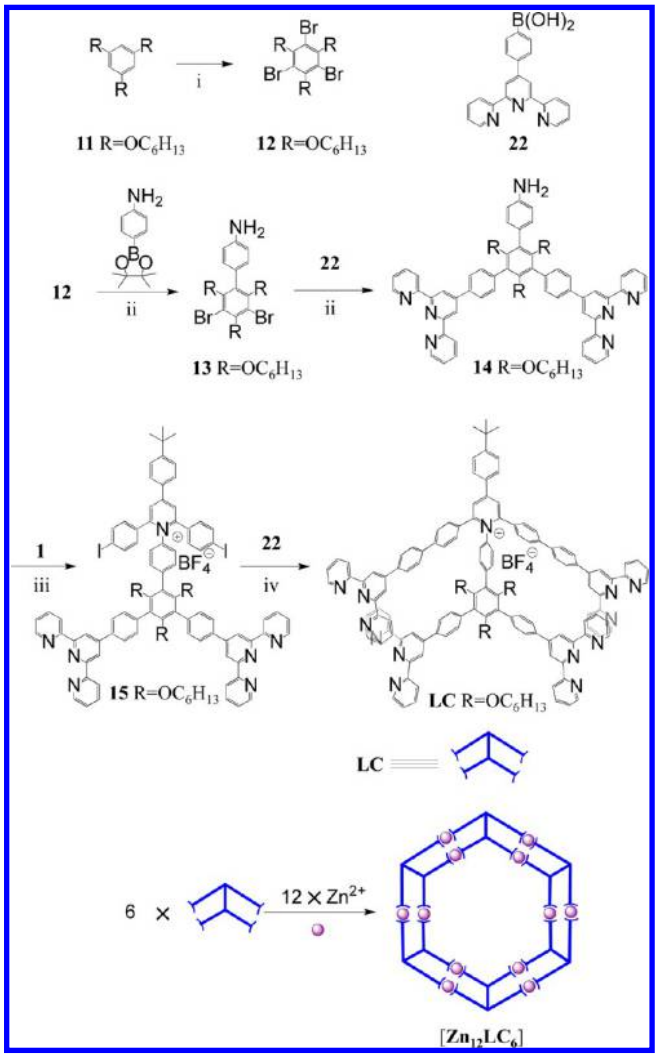

[a](i) $FeCl_3$, Br_2, $CHCl_3$; (ii) $Pd(PPh_3)_2Cl_2$, K_2CO_3, H_2O, toluene; (iii) NaOAc, ethanol; (iv) $Pd(PPh_3)_2Cl_2$, K_2CO_3, DMSO, H_2O.

It was expected to obtain a larger concentric hexagon. Similarly, the condensation reactions between pyrylium salt **1** and primary amine **14** were conducted to prepare pyridinium salt **15** for subsequent Suzuki coupling. After the coupling reaction, **LC** was purified through the same procedure as **LA** and **LB**, and characterized by ^{1}H NMR and MALDI-TOF mass spectrometry (Figures S16 and S20). The ^{1}H NMR pattern of ligand **LC** clearly showed the peaks of a3′,5′ and b3′,5′,

DOI: 10.1021/jacs.6b04959
J. Am. Chem. Soc. 2016, 138, 9258−9268

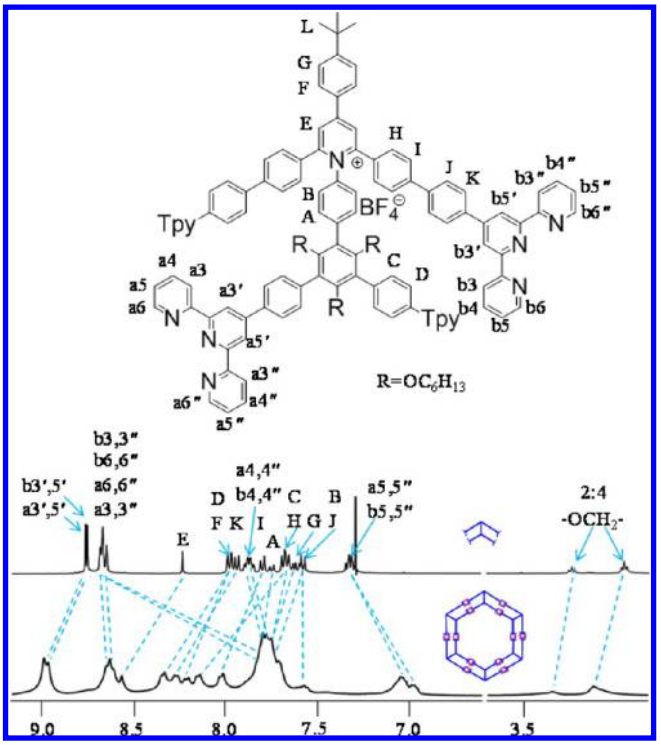

Figure 4. ^{1}H NMR spectra (400 MHz) of ligand **LC** in $CDCl_3$ and complex $[\mathbf{Zn_{12}LC_6}]$ in CD_3CN. The term "tpy" was used to replace the terpyridine structure.

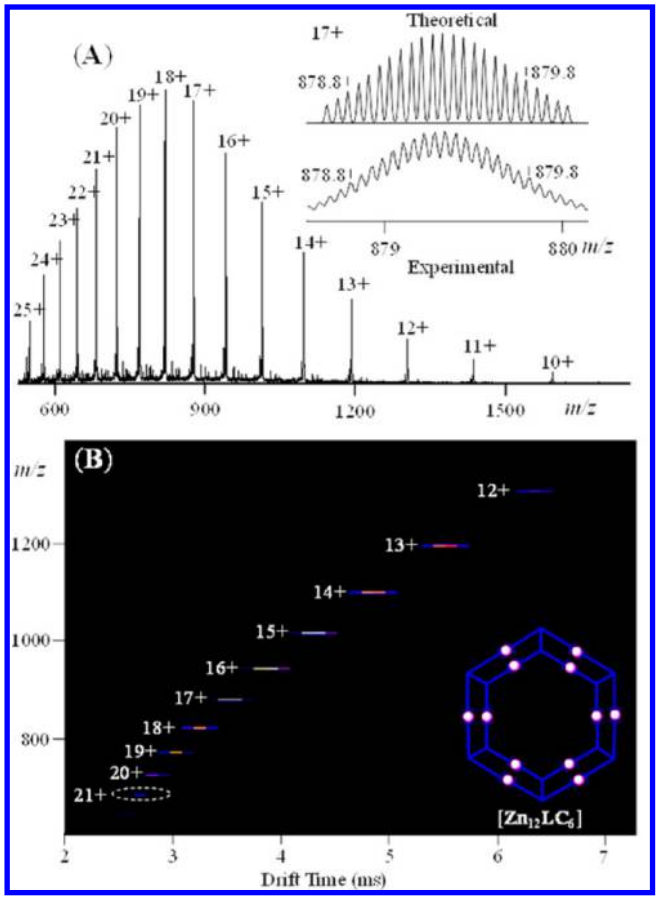

Figure 5. (A) ESI–MS and (B) 2D ESI–TWIM–MS plot (m/z vs drift time) of complex $[\mathbf{Zn_{12}LC_6}]$. The charge states of intact assemblies are marked.

Scheme 4. Synthesis of Ligand LD and Self-Assembly of Concentric Hexagon $[\mathbf{Zn_{12}LD_6}]$[a]

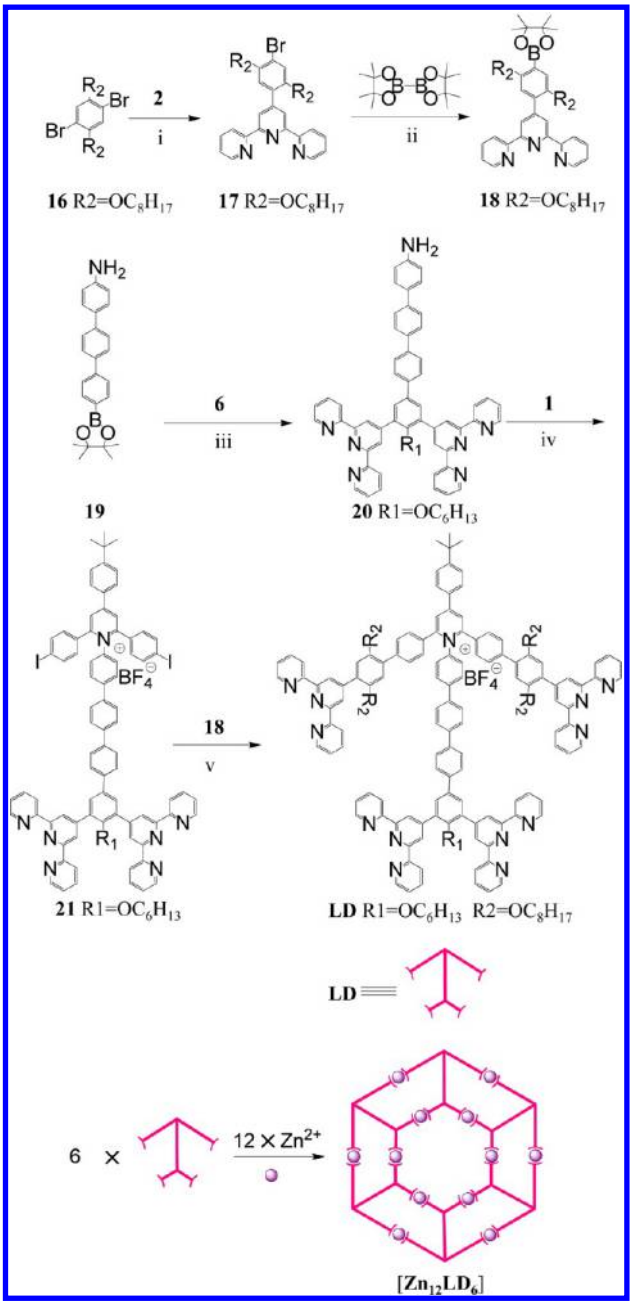

[a](i) $Pd(PPh_3)_2Cl_2$, K_2CO_3, toluene, H_2O; (ii) $Pd(dppf)Cl_2$, DMSO, KOAc; (iii) $Pd(PPh_3)_2Cl_2$, K_2CO_3, H_2O, toluene; (iv) NaOAc, ethanol; (v) $Pd(PPh_3)_2Cl_2$, K_2CO_3, DMSO, H_2O.

similar to those of ligand **LB**, suggesting the existence of two sets of tpy units.

Self-assembly of hexagon-in-hexagon $[\mathbf{Zn_{12}LC_6}]$ (yield 91%) followed the same procedure as complex $[\mathbf{Zn_{12}LB_6}]$. The ^{1}H NMR pattern of complex $[\mathbf{Zn_{12}LC_6}]$ with two sets of tpy signals (Figure 4) indicated the formation of a highly symmetric architecture. The 6,6″-tpy protons were shifted to upfield ($\Delta\delta$ = 0.9 ppm) upon complexation. More structural evidence was provided by 2D-COSY and NOESY (see Figures S34 and S35). The proton signals of alkoxy chain ($-OCH_2-$) also showed the expected ratio with aromatic protons as observed in complex $[\mathbf{Zn_{12}LB_6}]$.

DOI: 10.1021/jacs.6b04959
J. Am. Chem. Soc. 2016, 138, 9258–9268

Furthermore, ESI−MS and TWIM−MS spectra (Figure 5) of complex $[\mathbf{Zn_{12}LC_6}]$ identified one discrete species. The corresponding isotope patterns (in Figure S3) were in excellent agreement with calculated m/z isotopic distribution of concentric hexagon $[\mathbf{Zn_{12}LC_6}]$ with a molecular weight of 17 385.8 Da. The TWIM−MS spectrum (Figure 5B) also confirmed the absence of superimposed fragments, overlapping isomers, or structural conformers in this complex. All of these results suggested that we obtained a larger discrete concentric structure $[\mathbf{Zn_{12}LC_6}]$, indicating that the remarkable directing ability of tetratopic tpy ligand can be maintained within a longer arm.

Instead of increasing the size of both the inner and the outer rims, we attempted to elongate the spacer between two rims by introducing extra phenyl rings in the radial direction. As shown in Scheme 4, a spacer with three phenyl groups was applied in the synthesis of ditopic precursor **20** with primary amine for condensation reaction with pyrylium salt **1**. With the Suzuki coupling reaction, tetratopic ligand **LD** was obtained for self-assembly of concentric hexagon $[\mathbf{Zn_{12}LD_6}]$ (yield 88%) using the same assembly procedure (Figure 6). Because of the elongated

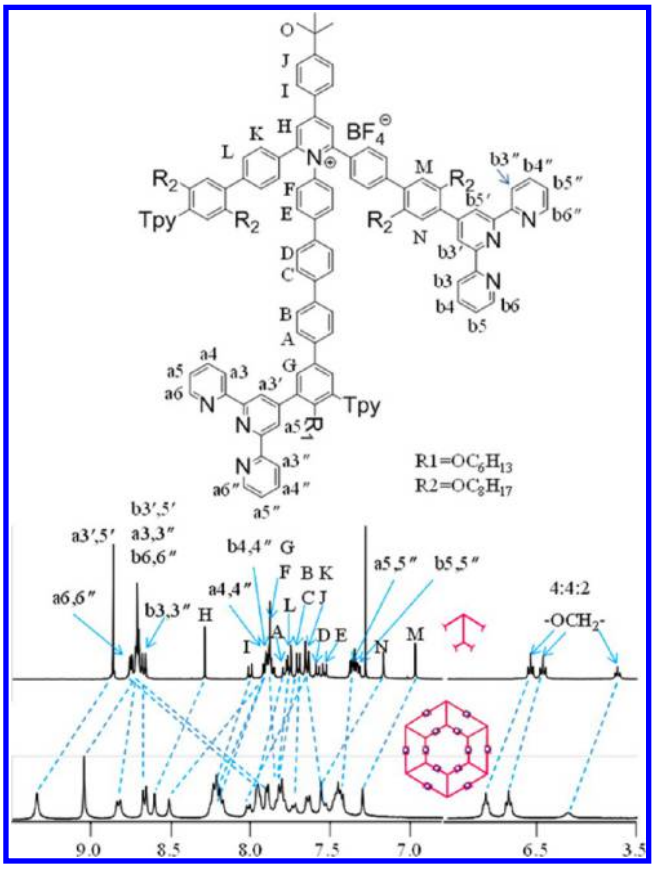

Figure 6. ^{1}H NMR spectra (400 MHz) of ligand **LD** in $CDCl_3$ and complex $[\mathbf{Zn_{12}LD_6}]$ in CD_3CN. The term "tpy" was used to replace the terpyridine structure.

three-phenyl spacer, the length difference between the arms of the inner and outer rims is two phenyls accordingly. The ^{1}H NMR spectrum of complex $[\mathbf{Zn_{12}LD_6}]$ was observed with two sets of tpy signals, and the alkoxy chain (−OCH_2−) also exhibited the expected ratio 4:4:2, suggesting the formation of discrete assembly. The structure was also confirmed by ESI−MS and TWIM−MS spectra with a molecular weight of 19 259.8 Da (Figure 7). The success of this series of concentric hexagons suggested that our design based on multitopic tpy

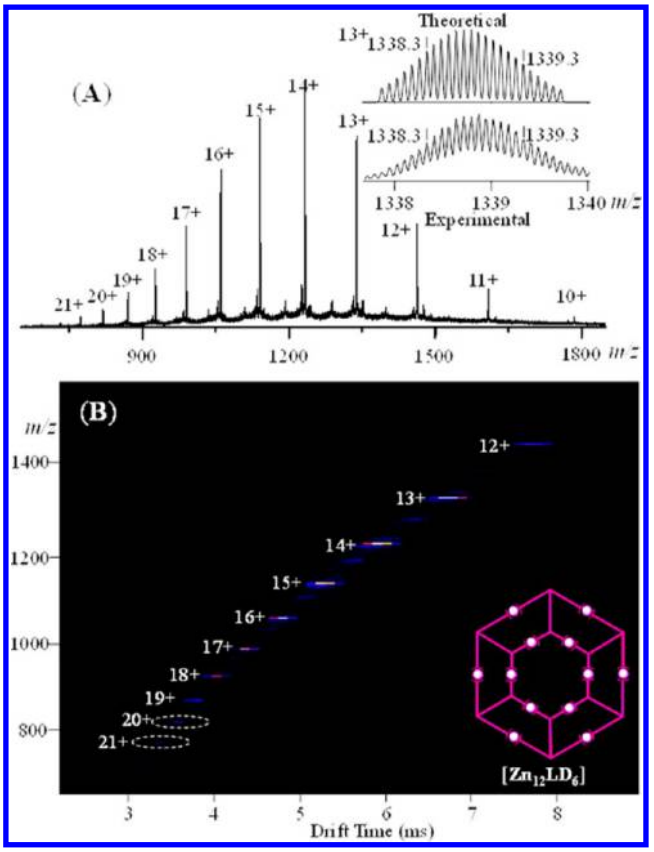

Figure 7. (A) ESI−MS and (B) 2D ESI−TWIM−MS plot (m/z vs drift time) of complex $[\mathbf{Zn_{12}LD_6}]$. The charge states of intact assemblies are marked.

ligands could become a robust strategy to assemble high generation of concentric hexagon.

Self-Assembly of Hybrid Concentric Hexagons. After the self-assembly of concentric hexagons using four tetratopic tpy ligands, our next question is whether we can assemble hybrid concentric hexagons to increase the diversity and complexity using the combination of ligands **LA**−**LD**. Considering the solubility and the matching of inner and outer rims of assembled concentric hexagons, **LB** and **LC** were chosen for the self-assembly of hybrid concentric hexagons. We reasoned that if **LB** and **LC** were mixed in an equimolar ratio accompanied by a stoichiometric amount of Zn(II) ions for self-assembly, we might obtain discrete $[\mathbf{Zn_{12}LB_3LC_3}]$ hybrid concentric hexagons by alternating **LB** and **LC** as shown in molecular moldeing (Figure 8C, middle). Following the same self-assembly procedure, ESI−MS was utilized to address the combination of equimolar ratio of **LB** and **LC** with Zn(II). In addition to the expected $[\mathbf{Zn_{12}LB_3LC_3}]$, another two hybrid concentric hexagons, that is, $[\mathbf{Zn_{12}LB_2LC_4}]$ and $[\mathbf{Zn_{12}LB_4LC_2}]$, were also observed as the major assemblies. The proposed molecular modeling structures of these two architectures were shown in Figure 8C. The isotope patterns of each charge states agreed well with the corresponding molecular composition (Figure 8B). However, optimization of different self-assembly prarameters, for example, temperature, sovlents, and counterions, to obtain single hexagon-in-hexagon $[\mathbf{Zn_{12}LB_3LC_3}]$ proved to be unsuccessful.

Size Characterization by 2D DOSY NMR, TWIM−MS, and TEM Imaging. Because of the large sizes and multiple long alkyl chains, it is challenging to grow a single crystal.

DOI: 10.1021/jacs.6b04959
J. Am. Chem. Soc. 2016, 138, 9258−9268

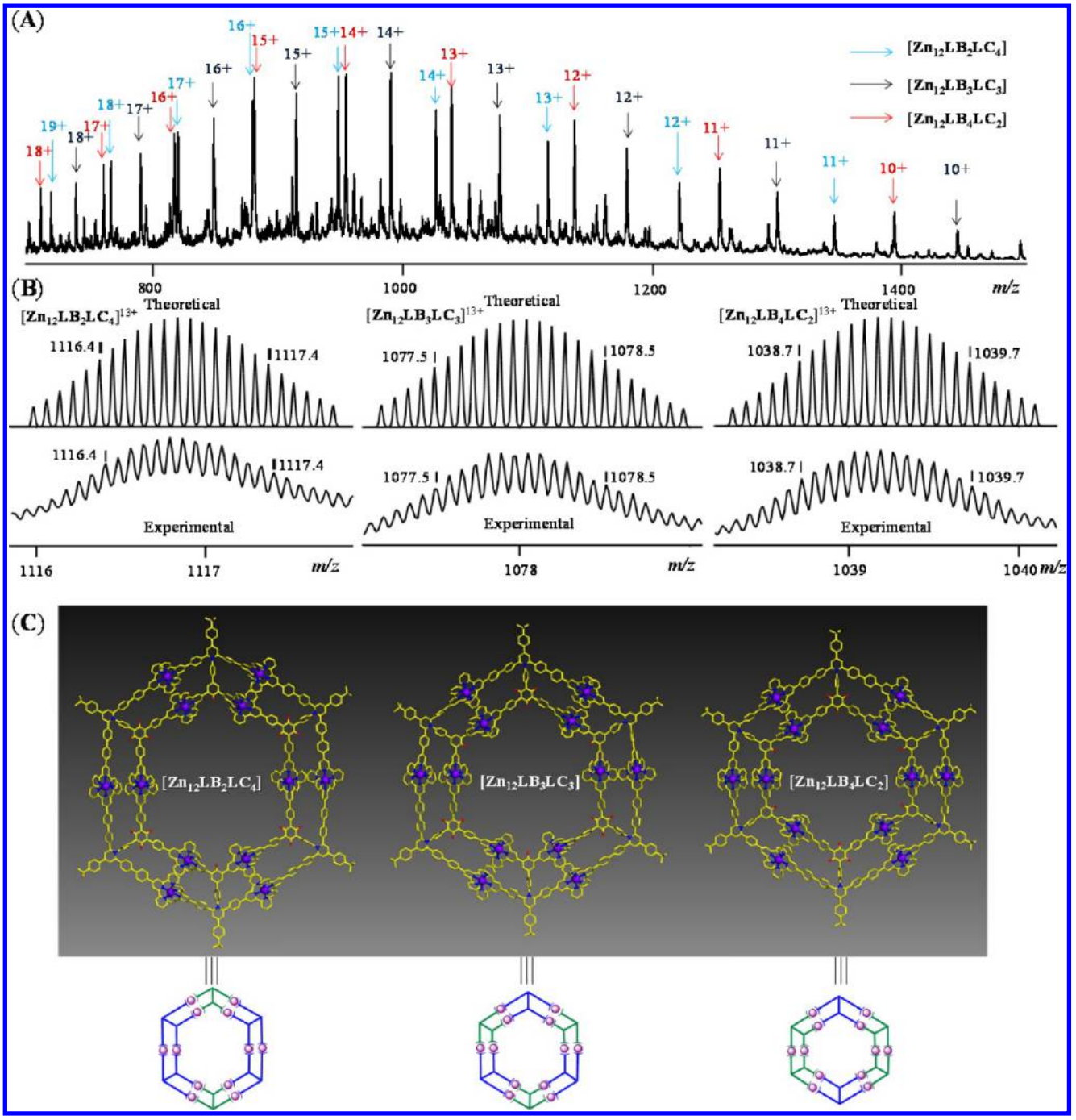

Figure 8. (A) ESI−MS of mixture of hybrid concentric hexagons. (B) The theoretical and experimental isotopic patterns of the 13+ signals. (C) Energy-minimized structures of $[\mathbf{Zn_{12}LB_2LC_4}]$, $[\mathbf{Zn_{12}LB_3LC_3}]$, and $[\mathbf{Zn_{12}LB_4LC_2}]$. The alkyl chains are omitted for clarity in the molecular modeling.

Nevertheless, 2D DOSY NMR was used to measure the trend of the size change as further evidence. As shown in Figure 9, we observed a single band at log D = −9.55, −9.78, and −9.85 for concentric hexagons $[\mathbf{Zn_{12}LB_6}]$, $[\mathbf{Zn_{12}LC_6}]$, and $[\mathbf{Zn_{12}LD_6}]$, respectively. Accordingly, the experimental hydrodynamic radii (r_H) of these complexes calculated via the Stokes−Einstein equation are 2.1, 3.6, and 4.2 nm, respectively.[23] As another strong evidence, collision cross sections (CCSs)[22] of analytes' ions were calculated from TWIM−MS data to correlate with the theoretical CCSs calculated from 70−100 candidate structures by molecular modeling for these concentric hexagon complexes. The experimental CCS deduced from TWIM−MS used the calibration curve as in a previous report.[25,26] The average experimental CCSs are 2021.1 ± 173.1, 2641.0 ± 198.3, and 2862.1 ± 159.8 Å^2 for $[\mathbf{Zn_{12}LB_6}]$, $[\mathbf{Zn_{12}LC_6}]$, and $[\mathbf{Zn_{12}LD_6}]$, respectively. As shown in Table 1, the theoretical CCSs calculated by the trajectory method using MOBCAL[27] are in good agreement with the average experimental CCSs.

On the basis of CCSs, the sizes of these concentric are similar to those of myoglobin. Because of their large sizes, we carried out TEM measurements of $[\mathbf{Zn_{12}LB_6}]$ and $[\mathbf{Zn_{12}LC_6}]$ by drop-casting dilute solutions onto Cu grid. TEM images shown in Figures 10, S44, and S45 revealed an individual particle with a weak contrast embedded in the thin film. The measured sizes

DOI: 10.1021/jacs.6b04959
J. Am. Chem. Soc. 2016, 138, 9258−9268

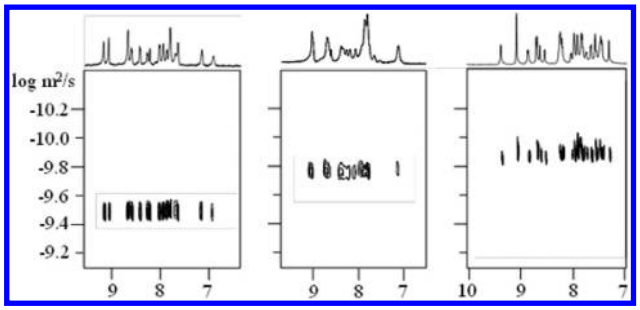

Figure 9. 2D DOSY NMR spectra of [$Zn_{12}LB_6$] (left), [$Zn_{12}LC_6$] (middle), and [$Zn_{12}LD_6$] (right) (500 Hz, CD_3CN, 300 K).

Table 1. Experimental and Theoretical Collision Cross Sections (CCSs)

	drift times [ms]	CCS [Å²]	CCS average [Å²]	CCS (calcd avg) [Å²]
[$Zn_{12}LB_6$]	6.06 (+9)	1815.2	2021.1 (173.1)	1907.7 ± 29.8
	5.07 (+10)	1843.1		
	4.30 (+11)	1878.9		
	3.75 (+12)	1934.2		
	3.31 (+13)	1995.4		
	2.98 (+14)	2068.3		
	2.76 (+15)	2129.6		
	2.54 (+16)	2210.4		
	2.32 (+17)	2316.5		
[$Zn_{12}LC_6$]	6.17 (+12)	2421.2	2641.0 (198.3)	2554.2 ± 44.1
	5.29 (+13)	2421.9		
	4.63 (+14)	2446.1		
	4.19 (+15)	2505.3		
	3.75 (+16)	2549.0		
	3.42 (+17)	2610.2		
	3.09 (+18)	2659.8		
	2.87 (+19)	2734.7		
	2.65(+20)	2801.9		
	2.54 (+21)	2902.1		
	2.43 (+22)	2998.5		
[$Zn_{12}LD_6$]	7.65(+12)	2699.4	2862.1 (159.8)	3018.9 ± 58.3
	6.62 (+13)	2723.5		
	5.73 (+14)	2716.5		
	5.07 (+15)	2736.7		
	4.63 (+16)	2795.9		
	4.19 (+17)	2839.6		
	3.86 (+18)	2902.7		
	3.64 (+19)	2991.2		
	3.42 (+20)	3071.9		
	3.20 (+21)	3144.8		

from TEM were comparable to the theoretical diameter of molecular modeling.

Hierarchical Self-Assembly of Supramolecular Metal–Organic Nanoribbons (SMON) at Solid/Liquid Interface. Previous studies reported that both intermolecular and molecule–substrate interactions could direct hierarchical self-assembly of preassembled metallo-supramolecules on solid surfaces to form 2D materials with promising magnetic, electronic, and photophysical properties.[28] We speculated that this series of giant 2D concentric hexagons with all rigid aromatic backbone should have strong $\pi-\pi$ interactions with highly oriented pyrolytic graphite (HOPG) surfaces according to a previous study.[29] Moreover, many previous studies extensively used alkylated compounds to obtain highly ordered assemblies of molecules

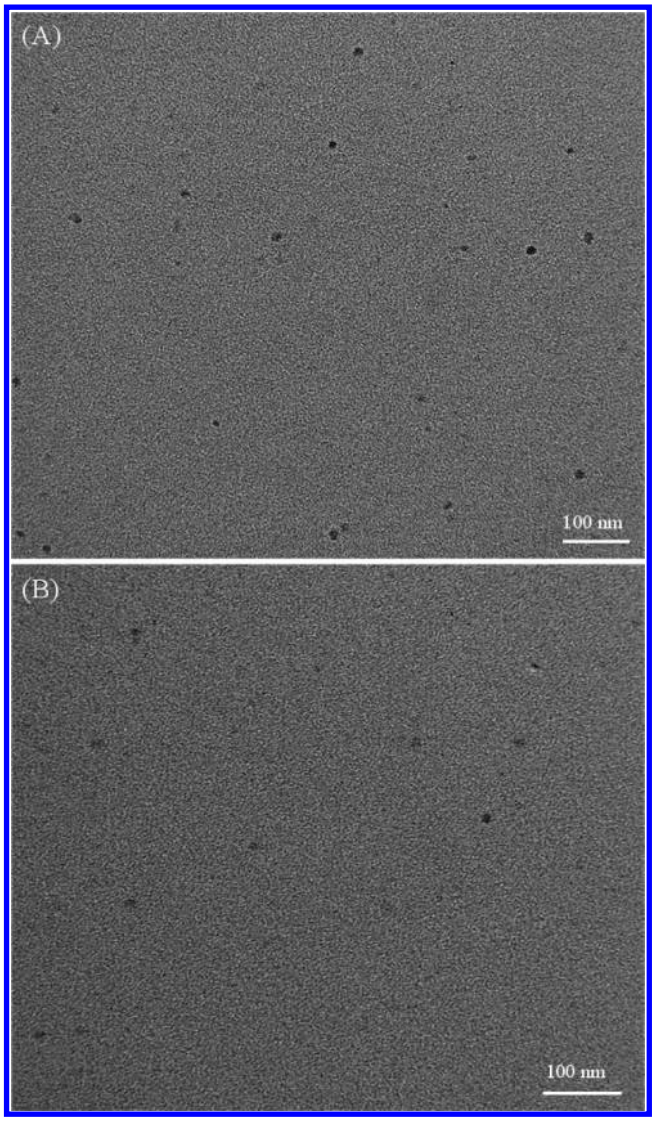

Figure 10. TEM images of complexes (A) [$Zn_{12}LB_6$] and (B) [$Zn_{12}LC_6$].

on HOPG surface by taking advantage of their high affinities for the surface of HOPG.[30] The high affinity originates from near commensurate packing of alkyl chains on the HOPG surface. In our designed concentric hexagons, multiple alkyl chains attached on the inner and/or outer rims of concentric hexagons not only increase solubility but also provide high affinities for HOPG surface. For instance, [$Zn_{12}LC_6$] has 18 $-OC_6H_{13}$ chains, and [$Zn_{12}LD_6$] has 24 $-OC_8H_{17}$ and 6 $-OC_6H_{13}$ chains connected to the rigid 2D structures. We herein investigated the hierarchical self-assembly of these two concentric hexagons on HOPG surface to deliver complex supramolecular materials.

Surprisingly, ambient STM imaging showed the formation of long 1D SMON rather than 2D assembly on the basal plane of HOPG surface after simple dropcasting of the solution of [$Zn_{12}LC_6$] onto a freshly cleaved surface of HOPG (Figure 11A–D; Figure S42). These single strand metal–organic nanoribbons were observed with monomer layer height and three-molecule width. The height of concentric nanoribbons is slightly larger than that of the aromatic ring because of the octahedral coordination geometry of the tpy-Zn(II)-tpy motif. Note that all of the black dots in the STM image are defects by missing concentric hexagon building blocks. In addition to the

DOI: 10.1021/jacs.6b04959
J. Am. Chem. Soc. 2016, 138, 9258–9268

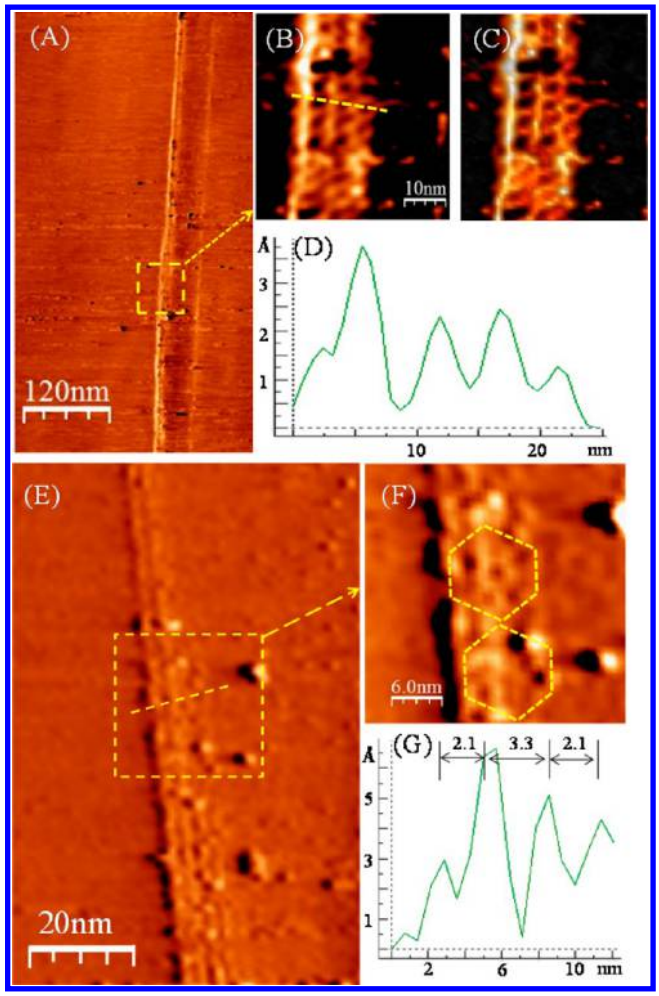

Figure 11. STM images of supramolecular metal−organic nanoribbons assembled by [$Zn_{12}LC_6$] (A−D) and [$Zn_{12}LD_6$] (E−G) on the HOPG surface.

formation of SMON, we also observed an individual concentric hexagon in STM imaging (Figure S42E−H).

Similarly, [$Zn_{12}LD_6$] also assembled into SMON at the liquid/solid interface with monomer layer height and single-molecule width (Figure 11E−G; Figure S43). One of the recent studies reported that inorganic nanowires of gold(I) cyanide could grow directly on pristine graphene, aligning themselves with the zigzag lattice directions of the graphene.[31] Our SMON assembled by [$Zn_{12}LC_6$] and [$Zn_{12}LD_6$] might grow along with zigzag or armchair lattice directions of graphene or random direction. If SMON was assembled along with either zigzag or armchair lattice, this direct alignment can be utilized to control crystallographic information about nanostructures, thus enabling us to fabricate SMON with specific directions. However, we were not able to get a high-resolution image for the lattice of HOPG using ambient STM in this study.

CONCLUSIONS

In summary, a series of concentric hexagons was assembled as discrete structures using tetratopic tpy ligands because of their high DOCS as compared to conventional self-assembly by ditopic tpy ligands. In preparation of tetratopic ligand, pyrylium and pyridinium salts' chemistry significantly facilitated synthesis. The key compounds were obtained by condensation reactions of pyrylium salts with corresponding primary amine derivatives in good yields. After self-assembly, these discrete metallo-supramolecular concentric hexagons were fully characterized by NMR, ESI−MS, TWIM−MS, and TEM, establishing their hexagon-in-hexagon architectures. The combination of different tetratopic ligands also assembled hybrid concentric hexagons with increasing diversity and complexity. The synthesis based on pyrylium and pyridinium salts chemistry together with the self-assembly strategy by increasing DOCS in this study will advance the design and self-assembly for more sophisticated 2D architectures in the future, such as high generation of concentric hexagon.

The success of these concentric hexagon supramolecules with precisely controlled shapes and sizes as building blocks paved an avenue toward complex functional materials through hierarchical self-assembly of SMON. It is expected that the high generation of concentric hexagons will have stronger $\pi-\pi$ interaction with the basal plane of HOPG surface, and thus assemble into highly ordered and uniform nanowires with less defects. This wet chemical method based on self-assembly offers simple, economical, and scalable routes to nanowires as compared to the various approaches being explored in the growth of semiconductor nanowires. Considering that semiconductor nanowires are emerging as a powerful class of materials for nanoscale photonic and electronic devices, SMON as an alternative will open substantial opportunities for electronic, sensing, and photonic applications, and their potential integration into more complex electronic and optoelectronic systems.

ASSOCIATED CONTENT

Supporting Information

The Supporting Information is available free of charge on the ACS Publications website at DOI: 10.1021/jacs.6b04959.

Experimental procedures and characterization data (PDF)

AUTHOR INFORMATION

Corresponding Authors

*xqhao@zzu.edu.cn
*bxu@engr.uga.edu
*x_l8@txstate.edu

Notes

The authors declare no competing financial interest.

ACKNOWLEDGMENTS

We gratefully acknowledge the support from NSF (CHE-1506722 and DMR-1205670), Research Corporation for Science Advancement (23224), ACS Petroleum Research Fund (55013-UNI3), and the National Natural Science Foundation of China (no. 21528201). Z.Z. thanks the China Scholarship Council for a graduate assistantship. We also acknowledge Dr. Chrys Wesdemiotis and Mr. Kevin Endres at the University of Akron for the MALDI-TOF measurements.

REFERENCES

(1) (a) Patel, S. S.; Picha, K. M. *Annu. Rev. Biochem.* **2000**, *69*, 651. (b) Lindoy, L. F.; Park, K.-M.; Lee, S. S. *Chem. Soc. Rev.* **2013**, *42*, 1713.

(2) (a) Cram, D. J. *Science* **1983**, *219*, 1177. (b) Cram, D. J. *Nature* **1992**, *356*, 29. (c) Hasenknopf, B.; Lehn, J.-M.; Kneisel, B. O.; Baum, G.; Fenske, D. *Angew. Chem., Int. Ed. Engl.* **1996**, *35*, 1838. (d) Bielawski, C. W.; Benitez, D.; Grubbs, R. H. *Science* **2002**, *297*, 2041.

(3) (a) O'Sullivan, M. C.; Sprafke, J. K.; V.Kondratuk, D.; Rinfray, C.; Claridge, T. D. W.; Saywell, A.; Blunt, M. O.; O'Shea, J. N.; Beton, P.

DOI: 10.1021/jacs.6b04959
J. Am. Chem. Soc. 2016, 138, 9258−9268

H.; Malfois, M.; Anderson, H. L. *Nature* **2011**, *469*, 72. (b) Sprafke, J. K.; Kondratuk, D. V.; Wykes, M.; Thompson, A. L.; Hoffmann, M.; Drevinskas, R.; Chen, W.-H.; Yong, C. K.; Kärnbratt, J.; Bullock, J. E.; Malfois, M.; Wasielewski, M. R.; Albinsson, B.; Herz, L. M.; Zigmantas, D.; Beljonne, D.; Anderson, H. L. *J. Am. Chem. Soc.* **2011**, *133*, 17262. (c) Kondratuk, D. V.; Perdigao, L. M. A.; O'Sullivan, M. C.; Svatek, S.; Smith, G.; O'Shea, J. N.; Beton, P. H.; Anderson, H. L. *Angew. Chem., Int. Ed.* **2012**, *51*, 6696. (d) Aggarwal, A. V.; Thiessen, A.; Idelson, A.; Kalle, D.; Würsch, D.; Stangl, T.; Steiner, F.; Jester, S.-S.; Vogelsang, J.; Höger, S. H.; Lupton, J. M. *Nat. Chem.* **2013**, *5*, 964. (e) Rousseaux, S. A. L.; Gong, J. Q.; Haver, R.; Odell, B.; Claridge, T. D. W.; Herz, L. M.; Anderson, H. L. *J. Am. Chem. Soc.* **2015**, *137*, 12713.

(4) (a) Fujita, M.; Yazaki, J.; Ogura, K. *J. Am. Chem. Soc.* **1990**, *112*, 5645. (b) Fujita, M.; Nagao, S.; Iida, M.; Ogata, K.; Ogura, K. *J. Am. Chem. Soc.* **1993**, *115*, 1574. (c) Fujita, M.; Ibukuro, F.; Hagihara, H.; Ogura, K. *Nature* **1994**, *367*, 720. (d) Stang, P. J.; Cao, D. H. *J. Am. Chem. Soc.* **1994**, *116*, 4981. (e) Stang, P. J.; Cao, D. H.; Saito, S.; Arif, A. M. *J. Am. Chem. Soc.* **1995**, *117*, 6273. (f) Stang, P. J.; Chen, K. *J. Am. Chem. Soc.* **1995**, *117*, 1667.

(5) (a) Caulder, D. L.; Raymond, K. N. *Acc. Chem. Res.* **1999**, *32*, 975. (b) Olenyuk, B.; Leininger, S.; Stang, P. J. *Chem. Rev.* **2000**, *100*, 853. (c) Holliday, B. J.; Mirkin, C. A. *Angew. Chem., Int. Ed.* **2001**, *40*, 2022. (d) Würthner, F.; You, C.-C.; Saha-Möller, C. R. *Chem. Soc. Rev.* **2004**, *33*, 133. (e) Fujita, M.; Tominaga, M.; Hori, A.; Therrien, B. *Acc. Chem. Res.* **2005**, *38*, 369. (f) Nitschke, J. R. *Acc. Chem. Res.* **2007**, *40*, 103. (g) Dalgarno, S. J.; Power, N. P.; Atwood, J. L. *Coord. Chem. Rev.* **2008**, *252*, 825. (h) Chakrabarty, R.; Mukherjee, P. S.; Stang, P. J. *Chem. Rev.* **2011**, *111*, 6810. (i) Smulders, M. M. J.; Riddell, I. A.; Browne, C.; Nitschke, J. R. *Chem. Soc. Rev.* **2013**, *42*, 1728. (j) Mukherjee, S.; Mukherjee, P. S. *Chem. Commun.* **2014**, *50*, 2239.

(6) Fujita, M.; Sasaki, O.; Mitsuhashi, T.; Fujita, T.; Yazaki, J.; Yamaguchi, K.; Ogura, K. *Chem. Commun.* **1996**, 1535.

(7) Schweiger, M.; Seidel, S. R.; Arif, A. M.; Stang, P. J. *Inorg. Chem.* **2002**, *41*, 2556.

(8) Weilandt, T.; Troff, R. W.; Saxel, H.; Rissanen, K.; Schalley, C. A. *Inorg. Chem.* **2008**, *47*, 7588.

(9) (a) Jiang, H.; Lin, W. *J. Am. Chem. Soc.* **2003**, *125*, 8084. (b) Jiang, H.; Lin, W. *J. Am. Chem. Soc.* **2004**, *126*, 7426. (c) Jiang, H.; Lin, W. *J. Am. Chem. Soc.* **2006**, *128*, 11286.

(10) (a) Leininger, S.; Fan, J.; Schmitz, M.; Stang, P. J. *Proc. Natl. Acad. Sci. U. S. A.* **2000**, *97*, 1380. (b) Olenyuk, B.; Levin, M. D.; Whiteford, J. A.; Shield, J. E.; Stang, P. J. *J. Am. Chem. Soc.* **1999**, *121*, 10434. (c) Olenyuk, B.; Whiteford, J. A.; Fechtenkotter, A.; Stang, P. J. *Nature* **1999**, *398*, 796. (d) Ghosh, K.; Hu, J.; White, H. S.; Stang, P. J. *J. Am. Chem. Soc.* **2009**, *131*, 6695. (e) Zheng, Y.-R.; Zhao, Z.; Kim, H.; Wang, M.; Ghosh, K.; Pollock, J. B.; Chi, K.-W.; Stang, P. J. *Inorg. Chem.* **2010**, *49*, 10238. (f) Zheng, Y.-R.; Lan, W.-J.; Wang, M.; Cook, T. R.; Stang, P. J. *J. Am. Chem. Soc.* **2011**, *133*, 17045. (g) Yan, X.; Cook, T. R.; Wang, P.; Huang, F.; Stang, P. J. *Nat. Chem.* **2015**, *7*, 342.

(11) (a) Tominaga, M.; Suzuki, K.; Kawano, M.; Kusukawa, T.; Ozeki, T.; Sakamoto, S.; Yamaguchi, K.; Fujita, M. *Angew. Chem., Int. Ed.* **2004**, *43*, 5621. (b) Sun, Q.-F.; Iwasa, J.; Ogawa, D.; Ishido, Y.; Sato, S.; Ozeki, T.; Sei, Y.; Yamaguchi, K.; Fujita, M. *Science* **2010**, *328*, 1144. (c) Sun, Q.-F.; Murase, T.; Sato, S.; Fujita, M. *Angew. Chem., Int. Ed.* **2011**, *50*, 10318. (d) Bunzen, J.; Iwasa, J.; Bonakdarzadeh, P.; Numata, E.; Rissanen, K.; Sato, S.; Fujita, M. *Angew. Chem., Int. Ed.* **2012**, *51*, 3161. (e) Sun, Q.-F.; Sato, S.; Fujita, M. *Nat. Chem.* **2012**, *4*, 330. (f) Sato, S.; Ikemi, M.; Kikuchi, T.; Matsumura, S.; Shiba, K.; Fujita, M. *J. Am. Chem. Soc.* **2015**, *137*, 12890. (g) Sawada, T.; Yamagami, M.; Ohara, K.; Yamaguchi, K.; Fujita, M. *Angew. Chem., Int. Ed.* **2016**, *55*, 4519. (h) Fujita, D.; Yokoyama, H.; Ueda, Y.; Sato, S.; Fujita, M. *Angew. Chem., Int. Ed.* **2015**, *54*, 155.

(12) (a) Mal, P.; Schultz, D.; Beyeh, K.; Rissanen, K.; Nitschke, J. R. *Angew. Chem., Int. Ed.* **2008**, *47*, 8297. (b) Hristova, Y. R.; Smulders, M. M. J.; Clegg, J. K.; Breiner, B.; Nitschke, J. R. *Chem. Sci.* **2011**, *2*, 638. (c) Meng, W.; Breiner, B.; Rissanen, K.; Thoburn, J. D.; Clegg, J. K.; Nitschke, J. R. *Angew. Chem., Int. Ed.* **2011**, *50*, 3479. (d) Meng, W.; Clegg, J. K.; Thoburn, J. D.; Nitschke, J. R. *J. Am. Chem. Soc.* **2011**, *133*, 13652. (e) Ousaka, N.; Clegg, J. K.; Nitschke, J. R. *Angew. Chem., Int. Ed.* **2012**, *51*, 1464. (f) Smulders, M. M. J.; Jiménez, A.; Nitschke, J. R. *Angew. Chem., Int. Ed.* **2012**, *51*, 6681. (g) Black, S. P.; Stefankiewicz, A. R.; Smulders, M. M. J.; Sattler, D.; Schalley, C. A.; Nitschke, J. R.; Sanders, J. K. M. *Angew. Chem., Int. Ed.* **2013**, *52*, 5749. (h) Bilbeisi, R. A.; Ronson, T. K.; Nitschke, J. R. *Angew. Chem., Int. Ed.* **2013**, *52*, 9027. (i) Castilla, A. M.; Ramsay, W. J.; Nitschke, J. R. *Acc. Chem. Res.* **2014**, *47*, 2063. (j) Ronson, T. K.; Roberts, D. A.; Black, S. P.; Nitschke, J. R. *J. Am. Chem. Soc.* **2015**, *137*, 14502. (k) Gan, Q.; Ronson, T. K.; Vosburg, D. A.; Thoburn, J. D.; Nitschke, J. R. *J. Am. Chem. Soc.* **2015**, *137*, 1770. (l) Wood, C. S.; Ronson, T. K.; Belenguer, A. M.; Holstein, J. J.; Nitschke, J. R. *Nat. Chem.* **2015**, *7*, 354. (m) Jansze, S. M.; Cecot, G.; Wise, M. D.; Zhurov, K. O.; Ronson, T. K.; Castilla, A. M.; Finelli, A.; Pattison, P.; Solari, E.; Scopelliti, R.; Zelinskii, G. E.; Vologzhanina, A. V.; Voloshin, Y. Z.; Nitschke, J. R.; Severin, K. *J. Am. Chem. Soc.* **2016**, *138*, 2046.

(13) (a) Hiraoka, S.; Harano, K.; Shiro, M.; Ozawa, Y.; Yasuda, N.; Toriumi, K.; Shionoya, M. *Angew. Chem., Int. Ed.* **2006**, *45*, 6488. (b) Hiraoka, S.; Harano, K.; Shiro, M.; Shionoya, M. *J. Am. Chem. Soc.* **2008**, *130*, 14368. (c) Hiraoka, S.; Yamauchi, Y.; Arakane, R.; Shionoya, M. *J. Am. Chem. Soc.* **2009**, *131*, 11646. (d) Clever, G. H.; Tashiro, S.; Shionoya, M. *J. Am. Chem. Soc.* **2010**, *132*, 9973.

(14) (a) Freye, S.; Hey, J.; Torras-Galán, A.; Stalke, Dietmar; Herbst-Irmer, D. R.; John, Michael; Clever, D. G. H. *Angew. Chem., Int. Ed.* **2012**, *51*, 2191. (b) Clever, G. H.; Kawamura, W.; Tashiro, S.; Shiro, M.; Shionoya, M. *Angew. Chem., Int. Ed.* **2012**, *51*, 2606. (c) Engelhard, D. M.; Freye, S.; Grohe, K.; John, M.; Clever, G. H. *Angew. Chem., Int. Ed.* **2012**, *51*, 4747. (d) Han, M.; Michel, R.; He, B.; Chen, Y.-S.; Stalke, D.; John, M.; Clever, G. H. *Angew. Chem., Int. Ed.* **2013**, *52*, 1319. (e) Freye, S.; Michel, R.; Stalke, D.; Pawliczek, M.; Frauendorf, H.; Clever, G. H. *J. Am. Chem. Soc.* **2013**, *135*, 8476. (f) Han, M.; Engelhard, D. M.; Clever, G. H. *Chem. Soc. Rev.* **2014**, *43*, 1848. (g) Löffler, S.; Lübben, J.; Krause, L.; Stalke, D.; Dittrich, B.; Clever, G. H. *J. Am. Chem. Soc.* **2015**, *137*, 1060. (h) Han, M.; Luo, Y.; Damaschke, B.; Gómez, L.; Ribas, X.; Jose, A.; Peretzki, P.; Seibt, M.; Clever, G. H. *Angew. Chem., Int. Ed.* **2016**, *55*, 445.

(15) (a) Ghosh, S.; Mukherjee, P. S. *J. Org. Chem.* **2006**, *71*, 8412. (b) Mahata, K.; Frischmann, P. D.; Würthner, F. *J. Am. Chem. Soc.* **2013**, *135*, 15656. (c) Lu, X.; Li, X.; Guo, K.; Xie, T.-Z.; Moorefield, C. N.; Wesdemiotis, C.; Newkome, G. R. *J. Am. Chem. Soc.* **2014**, *136*, 18149. (d) Wang, M.; Wang, C.; Hao, X.-Q.; Li, X.; Vaughn, T. J.; Zhang, Y.-Y.; Yu, Y.; Li, Z.-Y.; Song, M.-P.; Yang, H.-B.; Li, X. *J. Am. Chem. Soc.* **2014**, *136*, 10499. (e) Samanta, D.; Mukherjee, P. S. *Chem. - Eur. J.* **2014**, *20*, 12483. (f) Bhat, I. A.; Samanta, D.; Mukherjee, P. S. *J. Am. Chem. Soc.* **2015**, *137*, 9497. (g) Zhang, H.; Lee, J.; Lammer, A. D.; Chi, X.; Brewster, J. T.; Lynch, V. M.; Li, H.; Zhang, Z.; Sessler, J. L. *J. Am. Chem. Soc.* **2016**, *138*, 4573. (h) Wang, Q.-Q.; Gonell, S.; Leenders, S. H. A. M.; Dürr, M.; Ivanović-Burmazović, I.; Reek, J. N. H. *Nat. Chem.* **2016**, *8*, 225. (i) Cullen, W.; Misuraca, M. C.; Hunter, C. A.; Williams, N. H.; Ward, M. D. *Nat. Chem.* **2016**, *8*, 231. (j) Roy, B.; Zangrando, E.; Mukherjee, P. S. *Chem. Commun.* **2016**, *52*, 4489. (k) Li, K.; Zhang, L.-Y.; Yan, C.; Wei, S.-C.; Pan, M.; Zhang, L.; Su, C.-Y. *J. Am. Chem. Soc.* **2014**, *136*, 4456. (l) Wu, K.; Li, K.; Hou, Y.-J.; Pan, M.; Zhang, L.-Y.; Chen, L.; Su, C.-Y. *Nat. Commun.* **2016**, *7*, 10487.

(16) (a) Fasting, C.; Schalley, C. A.; Weber, M.; Seitz, O.; Hecht, S.; Koksch, B.; Dernedde, J.; Graf, C.; Knapp, E.-W.; Haag, R. *Angew. Chem., Int. Ed.* **2012**, *51*, 10472. (b) Wang, M.; Wang, C.; Hao, X.-Q.; Liu, J.; Li, X.; Xu, C.; Lopez, A.; Sun, L.; Song, M.-P.; Yang, H.-B.; Li, X. *J. Am. Chem. Soc.* **2014**, *136*, 6664. (c) Sun, B.; Wang, M.; Lou, Z.; Huang, M.; Xu, C.; Li, X.; Chen, L.-J.; Yu, Y.; Davis, G. L.; Xu, B.; Yang, H.-B.; Li, X. *J. Am. Chem. Soc.* **2015**, *137*, 1556.

(17) (a) Schubert, U. S.; Eschbaumer, C. *Angew. Chem., Int. Ed.* **2002**, *41*, 2892. (b) Hofmeier, H.; Schubert, U. S. *Chem. Soc. Rev.* **2004**, *33*, 373. (c) Constable, E. C. *Chem. Soc. Rev.* **2007**, *36*, 246. (d) Constable, E. C. *Coord. Chem. Rev.* **2008**, *252*, 842. (e) De, S.; Mahata, K.; Schmittel, M. *Chem. Soc. Rev.* **2010**, *39*, 1555. (f) Wild, A.; Winter, A.; Schlütter, F.; Schubert, U. S. *Chem. Soc. Rev.* **2011**, *40*, 1459.

(18) (a) Yan, X.; Li, S.; Cook, T. R.; Ji, X.; Yao, Y.; Pollock, J. B.; Shi, Y.; Yu, G.; Li, J.; Huang, F.; Stang, P. J. *J. Am. Chem. Soc.* **2013**, *135*,

DOI: 10.1021/jacs.6b04959
J. Am. Chem. Soc. 2016, 138, 9258−9268

14036. (b) Yan, X.; Cook, T. R.; Pollock, J. B.; Wei, P.; Zhang, Y.; Yu, Y.; Huang, F.; Stang, P. J. *J. Am. Chem. Soc.* **2014**, *136*, 4460. (c) Chen, L.-J.; Zhao, G.-Z.; Jiang, B.; Sun, B.; Wang, M.; Xu, L.; He, J.; Abliz, Z.; Tan, H.; Li, X.; Yang, H.-B. *J. Am. Chem. Soc.* **2014**, *136*, 5993. (d) Li, Z.-Y.; Zhang, Y.; Zhang, C.-W.; Chen, L.-J.; Wang, C.; Tan, H.; Yu, Y.; Li, X.; Yang, H.-B. *J. Am. Chem. Soc.* **2014**, *136*, 8577. (e) Shi, Y.; Wang, M.; Ma, C.; Wang, Y.; Li, X.; Yu, G. *Nano Lett.* **2015**, *15*, 6276.

(19) (a) Fu, J.-H.; Lee, Y.-H.; He, Y.-J.; Chan, Y.-T. *Angew. Chem., Int. Ed.* **2015**, *54*, 6231. (b) Wang, S.-Y.; Fu, J.-H.; Liang, Y.-P.; He, Y.-J.; Chen, Y.-S.; Chan, Y.-T. *J. Am. Chem. Soc.* **2016**, *138*, 3651.

(20) (a) Lainé, P.; Bedioui, F.; Ochsenbein, P.; Marvaud, V.; Bonin, M.; Amouyal, E. *J. Am. Chem. Soc.* **2002**, *124*, 1364. (b) Lainé, P. P.; Bedioui, F.; Loiseau, F.; Chiorboli, C.; Campagna, S. *J. Am. Chem. Soc.* **2006**, *128*, 7510. (c) Fortage, J.; Peltier, C.; Nastasi, F.; Puntoriero, F.; Tuyèras, F.; Griveau, S.; Bedioui, F.; Adamo, C.; Ciofini, I.; Campagna, S.; Lainé, P. P. *J. Am. Chem. Soc.* **2010**, *132*, 16700. (d) Fortage, J.; Peltier, C.; Perruchot, C.; Takemoto, Y.; Teki, Y.; Bedioui, F.; Marvaud, V.; Dupeyre, G.; Pospísil, L.; Adamo, C.; Hromadová, M.; Ciofini, I.; Lainé, P. P. *J. Am. Chem. Soc.* **2012**, *134*, 2691.

(21) (a) Wu, D.; Zhi, L.; Bodwell, G. J.; Cui, G.; Tsao, N.; Müllen, K. *Angew. Chem., Int. Ed.* **2007**, *46*, 5417. (b) Wu, D.; Pisula, W.; Enkelmann, V.; Feng, X.; Müllen, K. *J. Am. Chem. Soc.* **2009**, *131*, 9620.

(22) (a) Ruotolo, B. T.; Benesch, J. L. P.; Sandercock, A. M.; Hyung, S.-J.; Robinson, C. V. *Nat. Protoc.* **2008**, *3*, 1139. (b) Chan, Y.-T.; Li, X.; Soler, M.; Wang, J.-L.; Wesdemiotis, C.; Newkome, G. R. *J. Am. Chem. Soc.* **2009**, *131*, 16395. (c) Brocker, E. R.; Anderson, S. E.; Northrop, B. H.; Stang, P. J.; Bowers, M. T. *J. Am. Chem. Soc.* **2010**, *132*, 13486. (d) Song, J.; Grün, C. H.; Heeren, R. M. A.; Janssen, H.-G.; van den Brink, O. F. *Angew. Chem., Int. Ed.* **2010**, *49*, 10168. (e) Thiel, J.; Yang, D.; Rosnes, M. H.; Liu, X.; Yvon, C.; Kelly, S. E.; Song, Y.-F.; Long, D.-L.; Cronin, L. *Angew. Chem.* **2011**, *123*, 9033. (f) Uetrecht, C.; Barbu, I. M.; Shoemaker, G. K.; van Duijn, E.; Heck, A. J. R. *Nat. Chem.* **2011**, *3*, 126. (g) Ujma, J.; Cecco, M. D.; Chepelin, O.; Levene, H.; Moffat, C.; Pike, S. J.; Lusby, P. J.; Barran, P. E. *Chem. Commun.* **2012**, *48*, 4423. (h) Scarff, C. A.; Snelling, J. R.; Knust, M. M.; Wilkins, C. L.; Scrivens, J. H. *J. Am. Chem. Soc.* **2012**, *134*, 9193.

(23) Chan, Y.-T.; Li, X.; Yu, J.; Carri, G. A.; Moorefield, C. N.; Newkome, G. R.; Wesdemiotis, C. *J. Am. Chem. Soc.* **2011**, *133*, 11967.

(24) Wang, J.-L.; Li, X.; Lu, X.; Hsieh, I.-F.; Cao, Y.; Moorefield, C. N.; Wesdemiotis, C.; Cheng, S. Z. D.; Newkome, G. R. *J. Am. Chem. Soc.* **2011**, *133*, 11450.

(25) (a) Chan, Y.-T.; Li, X.; Moorefield, C. N.; Wesdemiotis, C.; Newkome, G. R. *Chem. - Eur. J.* **2011**, *17*, 7750. (b) Wang, J.-L.; Li, X.; Lu, X.; Chan, Y.-T.; Moorefield, C. N.; Wesdemiotis, C.; Newkome, G. R. *Chem. - Eur. J.* **2011**, *17*, 4830. (c) Li, X.; Chan, Y.-T.; Casiano-Maldonado, M.; Yu, J.; Carri, G. A.; Newkome, G. R.; Wesdemiotis, C. *Anal. Chem.* **2011**, *83*, 6667.

(26) Thalassinos, K.; Grabenauer, M.; Slade, S. E.; Hilton, G. R.; Bowers, M. T.; Scrivens, J. H. *Anal. Chem.* **2009**, *81*, 248.

(27) (a) Shvartsburg, A. A.; Jarrold, M. F. *Chem. Phys. Lett.* **1996**, *261*, 86. (b) Shvartsburg, A. A.; Liu, B.; Siu, K. W. M.; Ho, K.-M. J. *Phys. Chem. A* **2000**, *104*, 6152. (c) Jarrold, M. F. *Annu. Rev. Phys. Chem.* **2000**, *51*, 179.

(28) (a) Gong, J.-R.; Wan, L.-J.; Yuan, Q.-H.; Bai, C.-L.; Jude, H.; Stang, P. J. *Proc. Natl. Acad. Sci. U. S. A.* **2005**, *102*, 971. (b) Jeong, K. S.; Kim, S. Y.; Shin, U.-S.; Kogej, M.; Hai, N. T. M.; Broekmann, P.; Jeong, N.; Kirchner, B.; Reiher, M.; Schalley, C. A. *J. Am. Chem. Soc.* **2005**, *127*, 17672.

(29) (a) Li, S.-S.; Yan, H.-J.; Wan, L.-J.; Yang, H.-B.; Northrop, B. H.; Stang, P. J. *J. Am. Chem. Soc.* **2007**, *129*, 9268. (b) Chen, T.; Pan, G.-B.; Wettach, H.; Fritzsche, M.; Höger, S.; Wan, L.-J.; Yang, H.-B.; Northrop, B. H.; Stang, P. J. *J. Am. Chem. Soc.* **2010**, *132*, 1328.

(30) (a) de Feyter, S.; de Schryvera, F. C. *Chem. Soc. Rev.* **2003**, *32*, 139. (b) Otsuki, J. *Coord. Chem. Rev.* **2010**, *254*, 2311.

(31) Lee, W. C.; Kim, K.; Park, J.; Koo, J.; Jeong, H. Y.; Lee, H.; Weitz, D. A.; Zettl, A.; Takeuchi, S. *Nat. Nanotechnol.* **2015**, *10*, 423.

DOI: 10.1021/jacs.6b04959
J. Am. Chem. Soc. 2016, 138, 9258−9268